

INFLUENCE OF BALL MILLING PROCESS ON STRUCTURAL AND MAGNETIC PROPERTIES OF $\text{La}_{0.7}\text{Sr}_{0.3}\text{MnO}_3$ MANGANITE

✉ GLORIA CAMPILLO FIGUEROA¹
ÓSCAR ARNACHE OLMOS²
ANDRÉS GIL GARCÉS³
JAIME ALBERTO OSORIO VÉLEZ⁴
JAILES JOAQUÍN BELTRÁN⁵
EVAL BACA MIRANDA⁶
ROBERTO CASTILLO⁷

ABSTRACT

This investigation presents the magnetic and structural properties of ferromagnetic manganite $\text{La}_{0.7}\text{Sr}_{0.3}\text{MnO}_3$, (LSMO), subjected to ball milling processes. The LSMO powder sample was obtained by solid state reaction from high purity precursors. From X-ray diffraction (XRD), the sample showed the characteristic peaks of this phase. By means of thermogravimetric analysis (TGA) assisted by magnetic field, used as first method to measure the Curie temperature T_c , the NM (non-milling) LSMO powders exhibited a $T_c=369.69$ K (96.96 °C), which agrees with the magnetization measurements. In order to study size dependent properties, LSMO powder was subjected to mechanical milling processes during 3, 6 and 12 hours. From Rietveld refinement of XRD patterns, a reduction in crystallite average size (D_v) and a stabilization of crystalline structure (the R3c space group), with milling time (tM), were observed. These results are consistent with the Scanning Electron Microscopy (SEM) images, which showed more homogeneity in the grain distribution with longer milling times. From magnetic characterization results, it was found that the saturation magnetization decreases with decreasing grain size (smaller D_v). This behavior is attributed to surface effects that induce magnetically disordered states in smaller particle sizes. However, the T_c is kept constant around 365 K and it is independent of tM .

KEYWORDS: Manganites; Colossal Magnetoresistance; Nanoparticles; Magnetic Properties.

- 1 Física, Mg. y PhD. en Ciencias-Física, Universidad del Valle. Profesora e investigadora tiempo completo, Departamento de Ciencias Básicas, Universidad de Medellín, Medellín (Colombia).
- 2 Físico, Mg. y PhD. en Física, Universidad de Antioquia. Profesor e investigador Grupo de Estado Sólido, Universidad de Antioquia, Medellín (Colombia).
- 3 Estudiante de Ingeniería Química, Universidad de Antioquia. Grupo de Estado Sólido, Universidad de Antioquia, Medellín (Colombia).
- 4 Físico, Universidad de Antioquia; Mg. y PhD. en Física, Universidad del Valle. Profesor e investigador Grupo de Estado Sólido, Universidad de Antioquia, Medellín (Colombia).
- 5 Químico, Mg. en Ciencias Químicas y candidato a PhD. Universidad de Antioquia. Grupo de Estado Sólido, Universidad de Antioquia, Medellín (Colombia).
- 6 Físico, Mg. y PhD. en Ciencias-Física, Universidad del Valle. Profesor e investigador tiempo completo, Departamento de Física, Universidad del Valle, Cali (Colombia).
- 7 Físico, Mg. y PhD. en Ciencias-Física, Universidad del Valle. Profesor e investigador, Departamento de Física, Universidad del Valle, Cali (Colombia).

✉ Autor de correspondencia Campillo-Figueroa, G.: Carrera 87
30-65; Tel: 340 54 42; Medellín.
Correo electrónico: gecampillo@udem.edu.co

Historia del artículo:
Artículo recibido: 26-XI-2013 / Aprobado: 05-I-2014
Disponible online: 12 de mayo de 2014
Discusión abierta hasta mayo de 2015

INFLUENCIA DEL PROCESO DE MOLIENDA EN LAS PROPIEDADES ESTRUCTURALES Y MAGNETICAS DE MANGANITAS $\text{La}_{0.7}\text{Sr}_{0.3}\text{MnO}_3$

RESUMEN

Este trabajo estudia las propiedades estructurales y magnéticas de la manganita $\text{La}_{0.7}\text{Sr}_{0.3}\text{MnO}_3$ (LSMO) obtenida por el método de reacción en estado sólido y sometida a procesos de molienda mecánica. En las medidas de difracción de rayos X, XRD, la muestra en polvo de LSMO presentó los picos característicos de esta fase. La técnica de termogravimetría (TGA) asistida con campo magnético, mostró una temperatura de Curie $T_c = 369,69 \text{ K}$ ($=96,96 \text{ }^\circ\text{C}$). Este resultado concuerda con la temperatura de la transición magnética, cercana a 365 K . Con el fin de analizar la dependencia de las propiedades magnéticas y estructurales en relación con el tamaño de partícula, las muestras se sometieron a molienda mecánica por 3, 6 y 12 horas. A partir de refinamiento Rietveld de los rayos X, se observó una reducción de tamaño de partícula y una estabilización de la estructura cristalina de grupo espacial R3c, a medida que aumenta el tiempo de molienda tM . Esto es consistente con las imágenes de SEM, que mostraron más homogeneidad de la distribución de tamaño a mayor tM . En las medidas de magnetización en función de la temperatura, se encontró que la magnetización de saturación decrece con la disminución de tamaño de grano (D_v pequeños). Este comportamiento es atribuido a estados magnéticamente desordenados que se generan en la superficie. Sin embargo, la temperatura crítica se mantiene constante alrededor de 365 K e independiente de tM .

PALABRAS CLAVES: manganitas; magnetorresistencia colosal; nanopartículas; propiedades magnéticas.

INFLUÊNCIA DE PROCESSO DE MOAGEM DE BOLAS SOBRE AS PROPRIEDADES ESTRUTURAIS E MAGNÉTICAS DE $\text{La}_{0.7}\text{Sr}_{0.3}\text{MnO}_3$

SUMÁRIO

Neste trabalho investigamos as propriedades magnéticas e estruturais do manganite ferromagnética $\text{La}_{0.7}\text{Sr}_{0.3}\text{MnO}_3$ (LSMO), quando é sujeito ao processo de moagem. Uma amostra de pó LSMO foi conseguida no estado sólido por reação a partir de precursor de grande pureza. A partir de difração com raios x (XRD), a amostra mostrou picos de características nesta etapa. Por meio de uma análise termogravimétrica (TGA), assistida por campo magnético, usada como primeiro método para medir as temperaturas Curie T_c , os pós LSMO NM (Non-milling) mostraram $T_c = 369.69 \text{ K}$ ($96.96 \text{ }^\circ\text{C}$), o que é conforme às medidas da magnetização. Para estudar as propriedades dependentes do tamanho, o pó LSMO foi sujeito ao processo mecânico de moagem durante 3, 6 e 12 horas. De acordo ao padrão de refinamento do XRD de Rietveld, a redução do tamanho médio em cristalitos (D_v) e a estabilização da estrutura cristalina (o grupo R3c space), com o tempo de moagem (tM), foi observado. Este resultado é coerente com as imagens do Scanning Electron Microscopy (SEM), que mostraram mais homogeneidade na distribuição dos grãos durante o processo de moagem. Encontrou-se com os resultados da caracterização magnética que a saturação da magnetização reduz com a redução do tamanho dos grãos (D_v menores). Este comportamento é característico dos efeitos da superfície que provoca estados de desordem magnéticos em partículas menores. Todavia, o T_c é mantido constante ao redor de 365 K e independente do tM .

PALAVRAS-CHAVE: Manganites; Magnetorresistência Colossal; Nano partículas; Propriedades Magnéticas.

INTRODUCTION

Research on the field of Colossal Magnetoresistance (CMR) manganites, has been a source of great interest both on fundamental and potential application aspects, in different areas such as: Spintronic, Magnetic Storage Systems, Magnetic Sensors, Solid State Refrigerators, etc.; (Salamon, M. B. and Jaime, M, 2001; Bibes, M. and Barthélémy, A., 2007). $\text{La}_{1-x}\text{A}_x\text{MnO}_3$ (A= Sr, Ca, Ba, etc.), perovskites, offer diverse physical properties depending on the doping concentration and A-site ionic radius. Many of these properties are explained by the double exchange mechanism DE, via the interaction between Mn^{4+} - Mn^{3+} ion pairs (Zener, C, 1951; Tokura, Y., 1999). Particularly, $\text{La}_{1-x}\text{Sr}_x\text{MnO}_3$ (LSMO), manganites, have received intense attention, due to the CMR effect, as well as their high Curie temperature (T_c) and conduction by spin-polarized and close lattice parameter with others compounds, depending on x concentration (Hueso, *et al.*, 2007). Properties of these systems are sensitive to size effect depending on the fabrication, in a single crystal, of thin films (lattice strain, interfaces effects) or powders (core-shell effects) (Kim, *et al.*, 2010; Kameli, P., 2008; Dyakonov *et al.* 2010). In the field of the nanometer range of LSMO powders, their properties strongly depend on the size and shape of the particle. Among the most important properties that are found in such materials at reduced scale, is the low field magnetoresistance (LFMR), with potential applications in the spin-polarized conduction electrons (Kameli, P. 2008). The spin disorder around grain boundaries produces a strong scattering centre for highly spin-polarized conduction electrons. The aligning of the spin to its original state by the application of moderated fields is an issue that is related with the grain size effect. According to some models, the core is metallic and ferromagnetic, while the shell is insulating and spin disordering (Savosta, *et al.*, 2004). LSMO nanopowders have been studied because of grain boundary effects, which have shown significant differences in their physical properties with respect to the bulk material, having very important applications (as Low Field Magnetoresistance - LFMR). A reduction of grain size was found to influence the magnetization and coercivity in these compounds. From the models proposed for describing these particular behaviors, it has been found that the structural disorder close to the grain

boundary, affects the double exchange (DE) mechanism due to its sensitivity to changes in the stoichiometric composition, vacancies, dislocations, etc. This produces magnetically disordered states on the surface of the grains (Kameli, P., 2006).

In this work we report a structural and magnetic analysis of $\text{La}_{0.7}\text{Sr}_{0.3}\text{MnO}_3$ (LSMO) powders, obtained by solid state reaction method, and subjected to mechanical ball milling. Models based on the contribution of the grain surface on the magnetization and coercivity and the dependence on the magnetic properties with the particle size are discussed.

EXPERIMENTAL DETAILS

In this work, pure phase of ferromagnetic manganite LSMO was obtained by a solid state reaction method. The mixture of high purity precursors MnO_2 (99.0 %), SrCO_3 (99.9 %) and La_2O_3 (98.0 %), was synthesized according to the appropriate stoichiometric molar amounts. The initial powder was subjected to thermal treatment at 900 °C for 12 hours and 1200 °C for 24 hours, with rates of heating and cooling of 5 °C/min and 20 °C/min respectively and maceration between intervals. With the purpose of homogenizing the powders an additional maceration process was used, and the compound was subjected to a final heat treatment at 1300 °C for 6 hours, to ensure the complete reaction of the precursors and the stabilization of the phase. Then, in order to reduce particle size, the LSMO powders were subjected to mechanical dry grinding in a planetary ball mill Fritsch PULVERISETTE 5. This process is carried out at air atmospheric conditions by using stainless-steel balls (of 4.58 g each), and with a ball-to-powder ratio of 20:1. In addition to these parameters, a rotational speed of 250 rpm (collision energy) and different milling times were evaluated. For this study, a set of 4 samples of LSMO was used: samples for times of 3, 6 and 12 hours of milling, and the sample without milling process from the precursor phase (NM LSMO). All powders were characterized structural, morphological and magnetically. The structure of the powders was analyzed by XRD with a Cu-K α radiation source; the morphology of the powder samples was observed with SEM (JEOL JSM-6490LV) and magnetic measurements were performed via vibrating-sample

magnetometer technique (VSM) with the physical properties measurement system (PPMS, Quantum Design). Additionally, to investigate the milling time effect on the powders, a distribution grain size was measured by using Dynamic Light Scattering (DLS) in a Malvern Mastersize 2000 particle size analyzer. XRD patterns were fitted by using Rietica Rietveld program, in order to obtain structural parameters and the mean particle diameters for each powder. A fast measure of the T_c , was taken using the TGA technique assisted with an external magnetic field. Magnetization as a function of temperature measurements was carried out under ZFC and FC regimens of 500 Oe in the temperature range between 5 K and 370 K. Lastly, hysteresis loops $M(H)$ were measured in the range of applied field of 5 kOe to -5 kOe.

RESULTS AND ANALYSIS

Refinement of the XRD patterns using the Rietveld method for the formed LSMO powders for each milling

Table 1. Summary of the refined structural parameters of LSMO samples with different milling times. Where V is the volume cell and χ^2 (chi-square) is the goodness of fit.

Refined unit cell parameters	Milling time (h)			
	0	3	6	12
R3c				
$a=b$ (Å)	5.5021	5.4986	5.4962	5.4979
c (Å)	13.3607	13.3509	13.3502	
V (Å) ³	350.2	349.6	349.3	345.6
D_v (nm)	82.7	36.8	26.5	20.9
Fraction (wt %)	84	90	94	100
Pnma				
a (Å)	5.4768	5.4951	5.5251	
b (Å)	7.7377	7.7088	7.7512	
c (Å)	5.5196	5.5249	5.5279	
V (Å) ³	233.9	234.0	236.7	
D_v (nm)	70.5	32.5	24.4	
Fraction (wt %)	16	10	6	
χ^2	1.31	1.14	1.21	1.32

Figure 1. (Color online). Rietveld refinement analysis of XRD patterns of LSMO samples with different milling times. Solid symbols are experimental data, while solid lines represent the fit. The lines below are the difference pattern. The inset shows the variation of the D_v for R3c and Pnma phases with t_M .

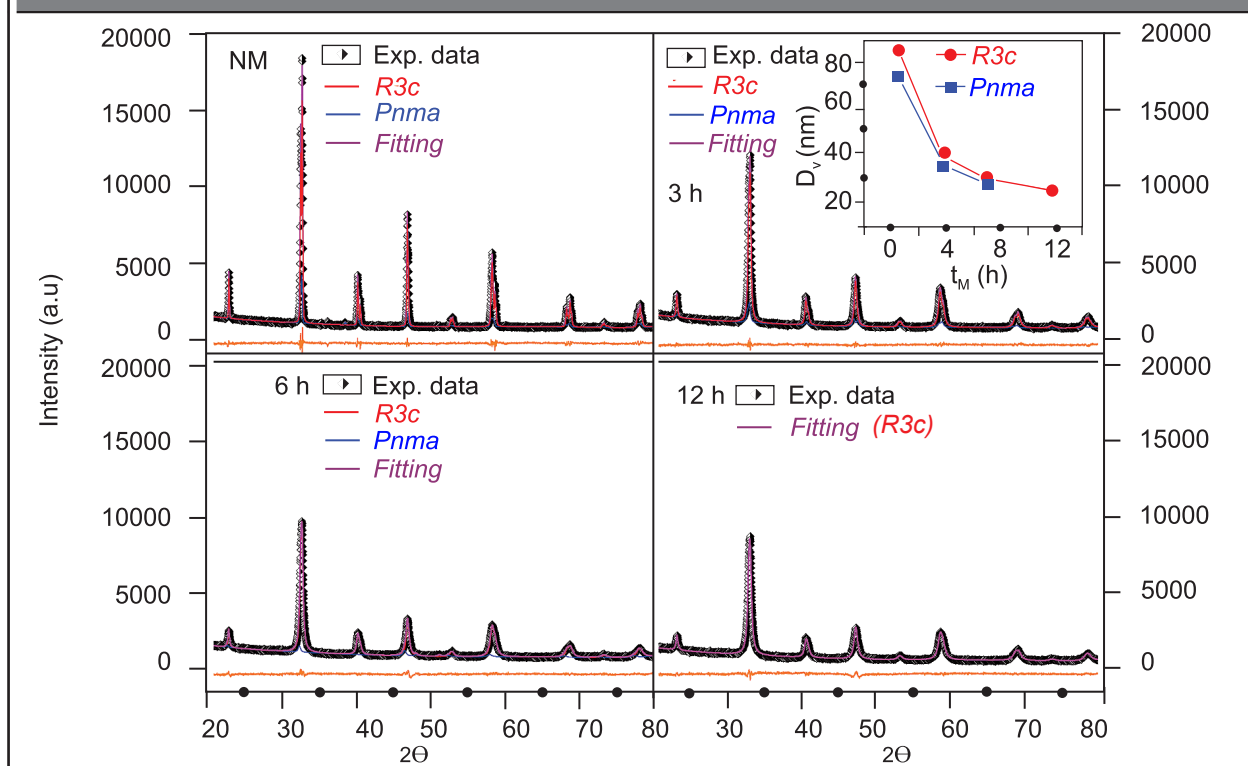
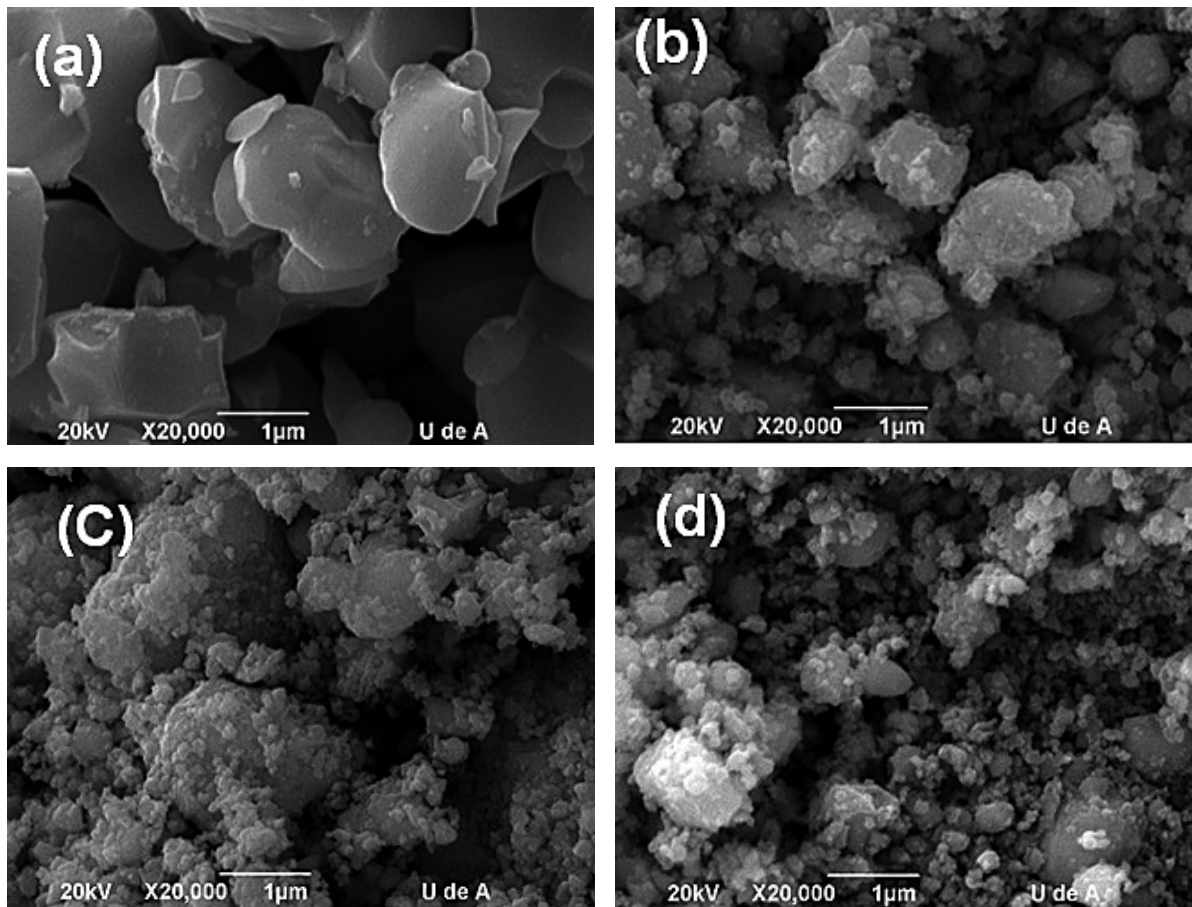


Figure 2. SEM micrograph for the LSMO samples, corresponding to (a) NM LSMO, (b) 3h, (c) 6h and (d) 12h.

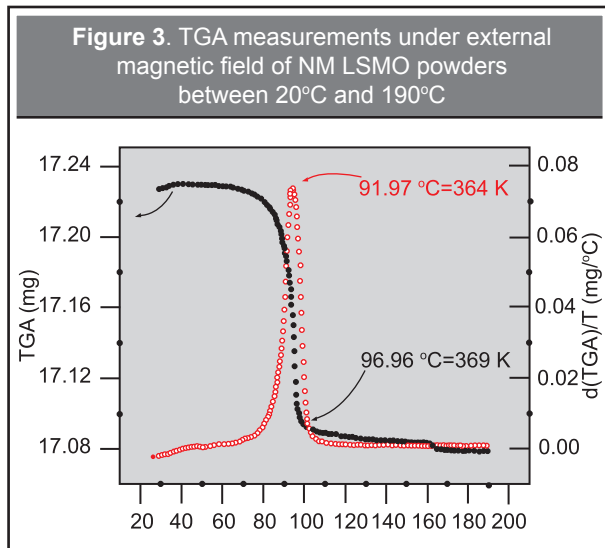


time are shown in **Figure 1**, and fitted lattice parameters are summarized in **Table 1**. XRD analysis for the NM LSMO sample reveals a mix of rhomboedral R3c and orthorhombic *Pnma* phases. With increasing milling time (3 and 6 h) a gradual conversion to R3c phase is observed, which appears as a single phase at time of 12 hours, see **Table 1**.

It is well known that mechanical milling processes can induce some microstrains in the system, and this may indicate diffusion at atomic level, which could lead to the production of non-equilibrium phases. Obviously, all of this depends on the milling conditions used in the experiment (ball material, milling time and rotational speed). From **Figure 1** it can be seen that the increasing of tM produces an increment in full width at half maximum (FWHM) and a decrease in the intensity of the diffraction peaks in comparison to the NM sample.

These changes indicate a reduction in the average crystallite size, D_v , and strain effects. When the R3c phase is consolidated, $tM = 12h$, the D_v is approximately 4 times smaller than the NM LSMO D_v (**Table 1**), which is associated with an increase in dislocation densities. In the inset of **Figure 1**, D_v is shown decreasing as a function of tM . Comparable results are reported for the $La_{0.8}Sr_{0.2}MnO_3$ compound prepared under similar conditions in Kameli (2006). According to these results, the milling process used for sample preparation can be considered crucial in the stabilization of the R3c phase. **Table 1** reports the decreasing of D_v for each tM , as well as the relative abundance (wt %), and the lattice parameters (a, b and c) of the R3c and *Pnma* phases.

Regarding the morphology of the samples, SEM micrographs of the milled and NM LSMO samples are shown in **Figure 2**, which also shows variations in



grain size distribution of LSMO as a function of milling time for the NM LSMO sample, and for 3, 6 and 12 hours of milling (according to DLS measurements, ranging from 900 to 100 nm approximately). Some differences between particle sizes are noticeable: the NM sample shows a distribution of larger grain size than the milled samples. Additionally, the EDX microanalysis confirmed the presence of each of the elements of these compounds.

The Thermogravimetric Analysis (TGA) assisted by magnetic field is a versatile and fast technique to obtain the critical temperature in ferromagnetic materials so it was used as a first method to measure the T_c of the initial LSMO powders. An amount of 17.23 mg of NM LSMO was placed on the TGA holder under an external magnetic field. If the material is ferromagnetic and does not experiment thermal weight losses, the apparent weight measured at $T < T_c$ is the sum of the real weight and the attraction force due to the magnetic field. In the transition region, that apparent weight falls abruptly up until the real weight. With this method NM LSMO powders were characterized in the temperature range between 20 °C and 190 °C as shown in **Figure 3**. The real weight obtained after the abrupt fall occurs at 96.96 °C (369.69 K), according to the magnetization data as a function of temperature, shown in **Figure 4**. The derivative of this curve with respect to temperature, has a maximum at 91.97 °C (364 K) corresponding to the inflexion point of the weight versus temperature data. In order to analyze in a rigorous way the magnetic behavior of these compounds, a VSM magnetometer was used.

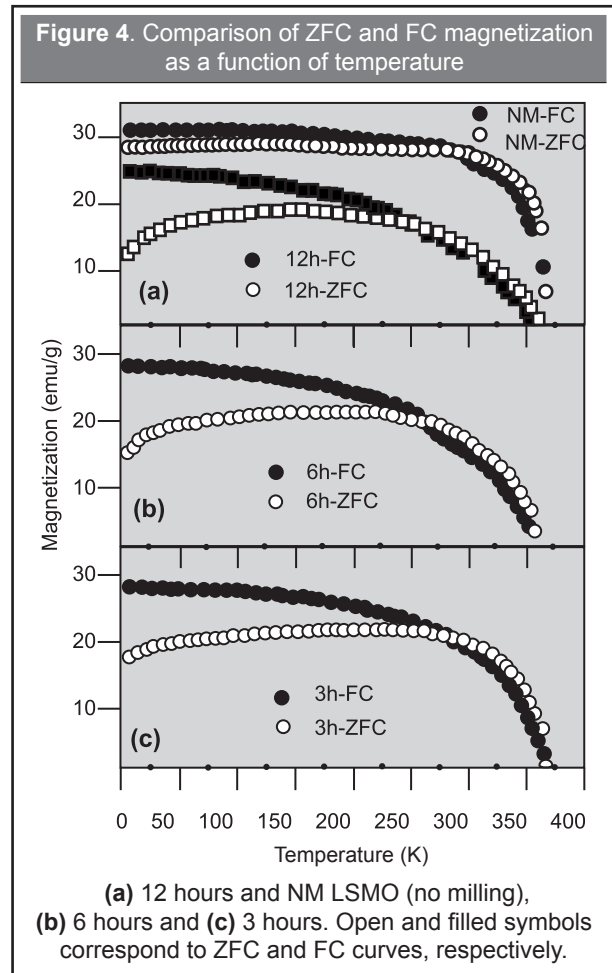
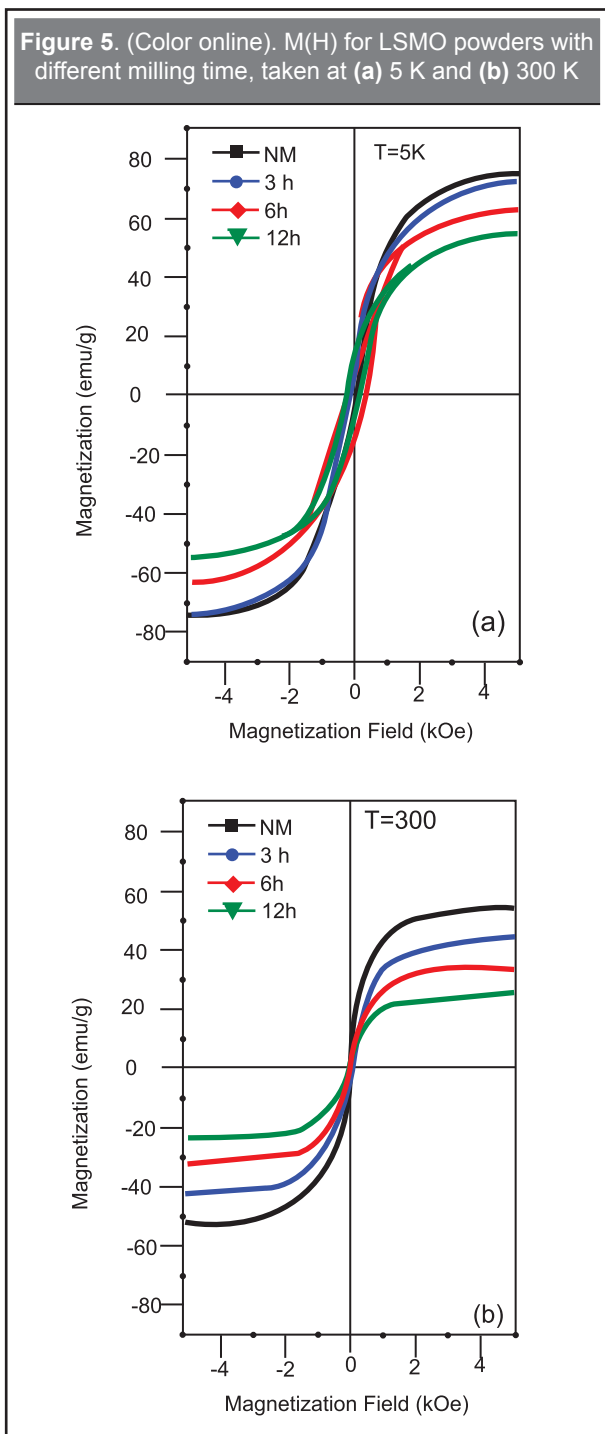
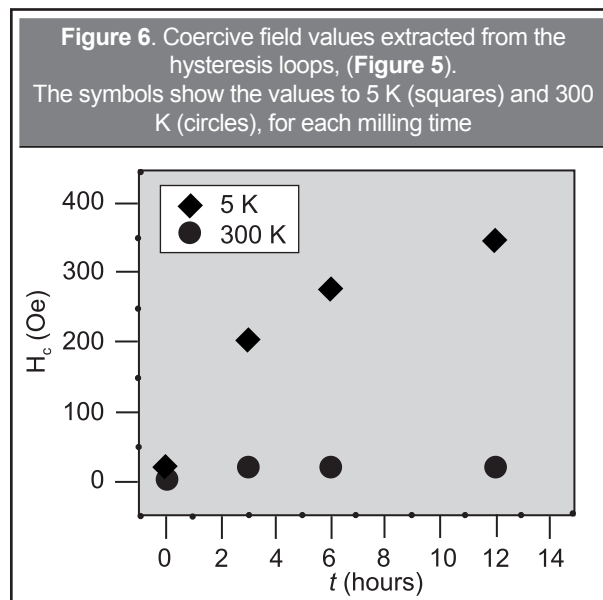


Figure 4 shows zero field cooling (ZFC) and field cooling (FC) magnetization measurements $M(T)$ for the NM LSMO powders and for the samples subjected to 3, 6 and 12 hours of milling. Both FC and ZFC curves were obtained with an external applied magnetic field of 500 Oe and exhibit a paramagnetic to ferromagnetic transition at ~ 365 K (extracted from the derivative of this curve) according to the TGA measurements. In general, an increase of the width of the magnetic transition and a decrease in the magnetization over all range of temperatures with milling time, are observed. **Figure 4(a)** shows how at low temperatures, the magnetization associated to ZFC and FC regimens decreases from ~ 28 emu/g (NM LSMO) to ~ 12 emu/g (12 hours), and from ~ 31 emu/g (NM LSMO) to 25 emu/g (12 hours), respectively. Additionally, the NM LSMO sample experiments saturation at low temperatures which does not occur in the LSMO sample milled for 12h. This



difference could be caused by a strong interaction between magnetic domains, characteristic of a harder ferromagnetic or a superparamagnetic behavior, which can be analyzed with the magnetization measurements as a function of magnetic field. A similar behavior was



observed in samples milled during 3 and 6 hours, **Figures 4(b) and 4(c)**.

Figure 5 shows the magnetization curves as a function of magnetic field $M(H)$ of the NM LSMO and LSMO samples milled during 3h, 6h and 12h, measured between -5 kOe and 5 kOe at 5 K (**Figure 5(a)**) and 300 K (**Figure 5(b)**). The NM LSMO sample shows a $M(H)$ curve without appreciable changes in its very small coercive fields and remanence at 5 K and 300 K due the decrease on the ferromagnetic contribution and the possibility of the presence of a superparamagnetic phase. In contrast, the milled LSMO samples clearly exhibit the evolution of coercive fields and remanence with temperature and milling time as presented in **Figure 6**. In this case, the coercive field increases with milling time at 5 K and decreases up to near zero values at 300 K. The decrease of this parameter is directly associated with a superparamagnetic behavior, which is enhanced in the LSMO sample milled during 12h. Hence, the milling process produces also a particle distribution of small size (nanoparticles) with superparamagnetic characteristics. This behavior can be attributed to magnetically disordered states at surface level, that appear when the grain experiments a size reduction, which induces, for example, some oxygen vacancies and strain effects that affect the $Mn^{3+} - O - Mn^{4+}$ bonds, and therefore ferromagnetic mechanisms, typical of these systems (Double Exchange) (Kameli, P., 2008). The saturation magnetization, M_s , presents a similar evolution. This is an evidence of the way that disordered states at the surface

can contribute to the behavior of particles with smaller sizes. The coercivity at 300 K is not affected by tM and is similar to that obtained at 5 K in all samples, indicating the dominant character of the superparamagnetic phase.

In summary, the milling process consolidates the R3c phase and produces very small LSMO particles that exhibit superparamagnetic properties. The coexistence of the ferromagnetic and superparamagnetic phases in these samples is manifest. The ferromagnetic phase is dominant at low temperatures in the milled samples and it is enhanced for the sample with $tM = 12\text{h}$, but at 300 K the dominant phase is of the superparamagnetic type.

ACKNOWLEDGEMENTS

This work was supported by the Sustainability Program for the Solid State Group 2010-2011, Universidad de Antioquia, Medellín. E. Baca and R. Castillo acknowledge the support to the Grupo de Ingeniería de Nuevos Materiales of the Universidad del Valle through Contract 7866-2011.

REFERENCES

- Bibes, M.; and Barthélémy, A. (2007). Oxide Spintronics, *IEEE Transactions on Electron Devices*, 54(5), pp. 1003-1023.
- Campillo, G.; Gil, A.; Arnache, O.; Beltrán, J. J.; Osorio, J. and Sierra, G. (2013). Analysis of Magnetic and Structural Properties in $\text{La}_{0.6}\text{Sr}_{0.4}\text{MnO}_3$ Ferromagnetic Particles under the Influence of Mechanical Ball Milling Effect. To be published in *Journal of Physics: Conference Series*.
- Dyakonov, V.; Slawska-Waniewska, A.; Nedelko, N.; Zubov, E.; Mikhaylov, V.; Piotrowski, K.; Szytula, A.; Baran, S.; Bazela, W. (2010). Magnetic, Resonance and Transport Properties of Nanopowder of $\text{La}_{0.7}\text{Sr}_{0.3}\text{MnO}_3$ Manganites. *Journal of Magnetism and Magnetic Materials*, 322(20) pp. 3072-3079.
- Hueso, L.E., et al. (2007). Transformation of Spin Information into Large Electrical Signals Using Carbon Nanotubes. *Nature* 445(January) pp. 410-413.
- Kameli, P.; Salamati, H. and Aezami, A. (2006). Effect of Particle Size on the Structural and Magnetic Properties of $\text{La}_{0.8}\text{Sr}_{0.2}\text{MnO}_3$. *Journal of Applied Physics*, 100 (5), pp. 053914 - 053914-4.
- Kameli, P.; Salamati, H. and Aezami, A. (2008). Influence of Grain Size on Magnetic and Transport Properties of Polycrystalline $\text{La}_{0.8}\text{Sr}_{0.2}\text{MnO}_3$ Manganites. *Journal Alloys and Compounds*, 450(1), pp. 7-11.
- Kim, Bongju; Kwon, Daeyoung; Song, Jong Hyun; Hikita, Yasuyuki; Kim, Bog G and Hwang, Harold Y. (2010). Finite Size Effect and Phase Diagram of Ultra-Thin $\text{La}_{0.7}\text{Sr}_{0.3}\text{MnO}_3$. *Solid State Commun*, 150(13-14), pp. 598-601.
- Salamon, M. B. and Jaime, M. (2001). The Physics of Manganites: Structure and Transport. *Reviews of Modern Physics*, 73(July), pp. 583-628.
- Savosta, M. M.; Krivoruchko, V. N.; Danilenko, I. A.; Tarenkov, V. Yu.; Konstantinova, T. E.; Borodin, A. V.; and Varyukhin, V. N. (2004). Nuclear Spin Dynamics and Magnetic Structure of Nanosized Particles of $\text{La}_{0.7}\text{Sr}_{0.3}\text{MnO}_3$. *Physical Review B*, 69, pp. 024413.
- Tokura, Y. *Colossal Magnetoresistive Oxides*. Tokyo: Gordon and Breach, 1999.
- Zener, C. (1951). Interaction between the d-Shells in the Transition Metals. II. Ferromagnetic Compounds of Manganese with Perovskite Structure. *Physical Review B*, 82(3) pp. 403-405.

**PARA CITAR ESTE ARTÍCULO /
TO REFERENCE THIS ARTICLE /
PARA CITAR ESTE ARTIGO /**

Campillo-Figueroa, G.; Arnache-Olmos, O.; Gil-Garcés, A.; Osorio-Vélez, J.A.; Beltrán, J. J.; Baca-Miranda, E.; Castillo, R. (2014). Influence of Ball Milling Process on Structural and Magnetic Properties of $\text{La}_{0.7}\text{Sr}_{0.3}\text{MnO}_3$ Manganite. *Revista EIA*, 11 (Edición especial N.1) marzo, pp. 31-38. [Online]. Disponible en: <http://dx.doi.org/10.14508/reia.2014.11.e1.31-38>